FEBS Letters 588 (2014) 705–712

FEBS Letters

journal homepage: www.FEBSLetters.org

Upregulated miR-106a plays an oncogenic role in pancreatic cancer

Pei Li [a,1], Qinhong Xu [a,1], Dong Zhang [a], Xuqi Li [b], Liang Han [a], Jianjun Lei [a], Wanxing Duan [a], Qingyong Ma [a], Zheng Wu [a], Zheng Wang [a,*]

[a] Department of Hepatobiliary Surgery, First Affiliated Hospital Medical College of Xi'an Jiaotong University, Xi'an, Shaanxi 710061, China
[b] Department of General Surgery, First Affiliated Hospital Medical College of Xi'an Jiaotong University, Xi'an, Shaanxi 710061, China

ARTICLE INFO

Article history:
Received 28 November 2013
Revised 31 December 2013
Accepted 3 January 2014
Available online 18 January 2014

Edited by Tamas Dalmay

Keywords:
Pancreatic cancer
miRNA
miR-106a
Cell invasion
Tissue inhibitors of metalloproteinase 2

ABSTRACT

Carcinogenesis is a complex process during which cells undergo genetic and epigenetic alterations. MicroRNAs control gene expression by negatively regulating protein-coding mRNAs. Several reports demonstrated that *miR-106a* is up-regulated in gastric and colorectal cancers and promotes tumor progression. In contrast, in glioma *miR-106a* plays the role of a tumor suppressor gene rather than an oncogene. Here we demonstrate that a high level of *miR-106a* expression is present in pancreatic cancer. Furthermore, our investigation shows that *miR-106a* has an oncogenic role in pancreatic tumorigenesis by promoting cancer cell proliferation, epithelial–mesenchymal transition and invasion by targeting tissue inhibitors of metalloproteinase 2 (*TIMP-2*). *MiR-106a* could be a critical therapeutic target in pancreatic cancer.
© 2014 Federation of European Biochemical Societies. Published by Elsevier B.V. All rights reserved.

1. Introduction

Carcinogenesis is a complex process during which cells undergo genetic and epigenetic alterations. MicroRNAs (miRNAs) are a class of endogenous, small noncoding RNAs that control gene expression by negatively regulating protein-coding mRNAs through base-pair matching with the 3′UTR [1]. In many tumors, miRNAs play critical roles, not only for diagnostic or prognostic indication [2–6] but also in cell proliferation, apoptosis, drug resistance and invasion [7–10].

One extensively studied miRNA is *miR-106a*. In 2013, Cui et al. found that *miR-106a* levels in gastric cancer tissues were significantly higher compared with the levels in normal adjacent tissues making *miR-106a* a potential biomarker that can assist in screening for gastric cancer [11]. Catela Ivkovic et al. found that *miR-106a* was overexpressed in samples from colorectal cancer patients compared with the adjacent normal tissues [12]. Several similar reports also demonstrated that *miR-106a* was up-regulated in the two tumors [13–16]. In contrast to gastric and colorectal cancers, Yang et al. [17] demonstrated that *miR-106a* was down-regulated in human glioma specimens and played the role of a tumor suppressor gene rather than an oncogene. Until now, little was known with respect to the potential regulatory mechanisms of *miR-106a* in pancreatic cancer, and the role *miR-106a* may play in pancreatic cancer has not been confirmed.

Based on previous reports, we investigated the expression pattern of *miR-106a* in pancreatic cancer by altering the endogenous levels of *miR-106a* in pancreatic cancer cell lines. We further investigated the role of *miR-106a* in proliferation, cell cycle progression, apoptosis and cell invasion in Panc-1 and SW-1990 cells. Direct targets of *miR-106a* were identified to elucidate the possible regulatory mechanism of *miR-106a* in pancreatic cancer.

2. Materials and methods

2.1. Tissue samples and cell cultures

All patients underwent radical surgical resection at the First Affiliated Hospital of Xi'an Jiaotong University. The specimens, which were immediately snap-frozen and stored at −80 °C in an ultra-low temperature refrigerator, were collected from 2010 to 2012. The frozen specimens, including pancreatic cancer and their matched non-tumor adjacent tissue samples, underwent pathological examination for confirmation and quantitative real-time PCR. This study was approved by the Ethical Committee of the First Affiliated Hospital of Medical College. Xi'an Jiaotong University, and written informed consent was obtained from all patients.

The human pancreatic cancer cell lines Panc-1, Miapaca-2, Bxpc-3, SW-1990 and HEK293 were obtained from the American

* Corresponding author. Fax: +86 29 85323899.
E-mail address: zheng.wang11@mail.xjtu.edu.cn (Z. Wang).
[1] These authors contributed equally to this work.

0014-5793/$36.00 © 2014 Federation of European Biochemical Societies. Published by Elsevier B.V. All rights reserved.
http://dx.doi.org/10.1016/j.febslet.2014.01.007

Type Culture Collection (Manassas, VA). All cells were cultured in Dulbecco's modified Eagle's medium (DMEM) containing 10% FBS, 100 units/ml of penicillin and 100 mg/ml of streptomycin. All cell lines were incubated at 37 °C in 5% CO_2.

2.2. Detection of mRNAs and miRNAs

Total RNA from pancreatic cancer cell lines and human tissue samples was extracted using the TRIzol reagent (Invitrogen, USA) according to the manufacturer's instructions, and 500 ng of each total RNA sample was utilized to synthesize cDNA using the PrimeScript® RT reagent Kit Perfect Real Time (TaKaRa, China). The quality and quantity of the total amount of RNA isolated was assessed in a NanoDrop Spectrophotometer by measuring the absorbance at 260 nm (A_{260}) and at 280 nm (A_{280}).

For mRNA detection and expression, tissue inhibitors of metalloproteinase 2 (*TIMP-2*), *E-cadherin*, *N-cadherin*, *vimentin* and *GAPDH* were analyzed by qRT-PCR. All qRT-PCR products were amplified using the SYBR Green Real-time PCR Master Mix (TaKaRa, China) following the manufacturer's instructions; amplicons were detected by an iQ5 Multicolor Real-Time PCR Detection System (Bio-Rad, Hercules, CA). *GAPDH* was used as the internal control for normalizing data in transfected cells. Fold changes in *TIMP-2* expression were quantified based on the ratio of *TIMP-2* mRNA/*GAPDH* mRNA using the $2^{-\Delta\Delta Ct}$ method, where $\Delta\Delta Ct = \Delta CtEX - \Delta CtNC = (CtEX\text{-}TIMP\text{-}2 - CtEX\text{-}GAPDH) - (CtNC\text{-}TIMP\text{-}2 - CtNC\text{-}GAPDH)$; "EX" represents the experimental group, and "NC" represents the negative control group. And fold changes of EMT hallmarkers expression were calculated through $2^{-\Delta\Delta Ct}$ method, where $\Delta\Delta Ct = \Delta CtCa - \Delta CtCp = (CtCa\text{-target gene} - CtCa\text{-}GAPDH) - (CtCp\text{-target gene} - CtCp\text{-}GAPDH)$; "Ca" represents the pancreatic cancer tissue, and "Cp" represents the non-tumor adjacent normal pancreas tissue. The PCR profile was one cycle at 95 °C for 5 min, followed by 40 cycles at 95 °C for 5 s, 58 °C for 30 s and 72 °C for 30 s. The primers used for detection are listed in Table 1.

For miRNA detection, we employed a stem-loop RT-PCR method using specific reverse transcription primers as previously described [18]. *U6* small nuclear RNA was used as the control to determine relative *miR-106a* expression, which was calculated using the $2^{-\triangle\triangle Ct}$ method. The PCR profile was one cycle at 95 °C for 5 min followed by 40 cycles at 95 °C for 5 s and 60 °C for 30 s. The primers used for detection are listed in Table 1.

2.3. Transfection

MiR-106a mimics, *miR-106a* inhibitors, siRNA-*TIMP2* (*TIMP2*-homo-418, *TIMP2*-homo-503 and *TIMP2*-homo-754) and negative control oligonucleotides were purified by high-performance liquid chromatography (GenePharma, China). The sequences were as follows: *miR-106a* mimics: 5′-AAAAGUGCUUACAGUGCAGGUAG-3′, *miR-106a* inhibitors: 5′-CUACCUGCACUGUAAGCACUUUU-3′, *TIMP2*-homo-418: 5′ GCAAUGCAGAUGUAGUGAUTT 3′, *TIMP2*-homo-503: 5′ GGAUCCAGUAUGAGAUCAATT 3′, *TIMP2*-homo-754: 5′ GCUGCGAGUGCAAGAUCACTT 3′ and negative controls: 5′-UUCUCCGAACGUGUCACGUTT-3′. Cells were transiently transfected with siRNA (100 nM), anti-miR inhibitors (100 nM) or mimics (50 nM) using Lipofectamine 2000 (Invitrogen, USA) following the manufacturer's instructions.

2.4. Cell viability assay

After transfection, cell viability was measured by the MTT assay in a time-dependent manner. Pancreatic cancer cells were plated into 96-well culture plates in triplicate prior to transfecting the cells with *miR-106a* mimics or *miR-106a* inhibitors and their negative controls. Then, the cells were cultured for 24, 48, 72 and 96 h. After transfection, 20 μl MTT (5 mg/ml) was added to each well, and incubated for 4 h at 37 °C. Following the removal of the supernatant, 150 μl of dimethyl sulfoxide (DMSO) was added to each well. Optical density (OD) was measured at the wavelength of 490 nm. The data are presented as the mean ± SD. Tests were performed in triplicate.

2.5. Apoptosis assay

The cells were seeded into 6-well plates and then transfected with *miR-106a* mimics or inhibitors and their negative controls. After 48 h, the cells were harvested, and the ratio of apoptosis was determined using the Annexin V Apoptosis Detection Kit according to the manufacturer's instructions. Apoptotic cells were examined and quantified by flow cytometry (FCM). Tests were performed in triplicate.

2.6. Cell cycle analysis

Cells were grown and transfected as mentioned above. Cell cycle phase was assessed by flow cytometry. Cells were collected, washed with phosphate-buffered saline (PBS) and fixed overnight in 75% ethanol at −20 °C, then treated with 25 μg/ml of DNase-free

Table 1
Primers of qRT-PCR.

Primers	Sequence
U6	F: CTCGCTTCGGCAGCACA
	R: AACGCTTCACGAATTTGCGT
miR-106a	RT: GTCGTATCCAGTGCGTGTCGTGGAGTCGGCAATTGCACTGGATACGACctacctg
	F: ATCCAGTGCGTGTCGTG
	R: TGCTAAAAGTGCTTACAGTG
GAPDH	F: CTCTGATTTGGTCGTATTGGG
	R: TGGAAGATGGTGATGGGATT
TIMP-2	F: GAACATCAACGGGCACCAG
	R: TCCCTCCAGACCCACAACC
E-cadherin	F: TGCTGTTTCTGGTTTCTGTTGG
	R: CCTTCTCCGTATTCTCCTCCCT
N-cadherin	F: TTTGGGGAGGGGTAAAAGTTC
	R: AAGAAACAGGCCACCCCTTT
Vimentin	F: CGGTTGAGACCAGAGATGGA
	R: TGCTGGTACTGCACTGTTGG

RNase A and stained with 50 μg/ml of propidium iodide at room temperature for 30 min. Tests were performed in triplicate.

2.7. Cell invasion analysis

Cell invasion was assayed using a chamber that was 6.5 mm in diameter, with an 8 μm pore size. At 48 h post-transfection, pancreatic cancer cells were suspended with serum-free medium and added to the upper chamber, which was coated with matrigel while 0.5 ml of 15% FBS-DMEM was added to the lower chamber. Cells were incubated for 24 h at 37 °C, and non-invading cells were removed with cotton swabs. Cells invading the bottom of the membrane were stained with 0.1% crystal violet for 30 min, and washed with PBS. Tests were performed in triplicate.

2.8. Western blotting

Total proteins were extracted from human pancreatic cancer cells with RIPA lysis buffer. Proteins were separated on 10% sodium dodecyl sulfate polyacrylamide gels, and the gels were transferred to PVDF membranes (Millipore, USA). The membranes were blocked overnight at 4 °C with 5% skimmed milk and then incubated with rabbit anti-human antibodies against *TIMP-2*/*MMP-2*/*MMP-9*/*E-cadherin*/*N-cadherin*/*Vimentin* (Santa Cruz Biotechnology, USA) or *GAPDH* (Cell Signaling, China). After washing, the membranes were incubated with goat anti-rabbit IgG at room temperature for 2 h. A chemiluminescence system (Millipore, USA) was used to detect specific binding.

2.9. Target prediction

TargetScan Release 5.2 (www.targetscan.org), a computational analysis tool, was used to predict targets of *miR-106a*, such as *TIMP-2*.

2.10. Luciferase reporter assay

The 3′-UTR sequence of *TIMP-2* predicted to interact with *miR-106a* or a mutated sequence within the predicted target sites was inserted into pEZX-MT01 target reporter plasmid constructs called WT-*TIMP-2* 3′UTR and MUT-*TIMP-2* 3′UTR, respectively. For the reporter assay, HEK-293 cells were plated into 24-well plates and transfected with the above constructs (0.5 μg) and *miR-106a* mimics (50 nM) or negative controls (50 nM) using the Lipofectamine 2000 reagent (Invitrogen, USA). After 48 h, the cells were harvested and assayed using the dual-Luciferase Reporter Assay system (Promega, USA) according to the manufacturer's instructions. For each sample, firefly luciferase activity was normalized to the renilla luciferase activity value. The experiment was performed in duplicate in three independent experiments.

2.11. Statistical analysis

Each experiment was conducted at least three times. All values were reported as the mean ± S.D. Differences were tested for significance using Student's *t*-test and One-way ANOVA analysis. Significant association between *miR-106a* and EMT hallmarkers mRNA expression was assessed by a Fisher exact test. $P < 0.05$ was considered a statistically significant difference.

3. Results

3.1. MiR-106a levels were elevated in human pancreatic cancer and altered after transfection

Expression levels of *miR-106a* were detected from 21 human pancreatic cancer samples using qRT-PCR. We found that the expression of *miR-106a* was significantly higher in PDAC tissues than in paired adjacent normal pancreatic tissues (Fig. 1A). The *miR-106a* expression level was increased more than 2-fold in 16 (76.19%) tumor samples with an average increase of 5.12 fold.

Of the four pancreatic cancer cell lines, the highest expression of *miR-106a* was detected in the SW-1990, a spleen metastasis cell line (Fig. 1B). Furthermore, we also found that with the enhancement of cell invasiveness, the level of *miR-106a* gradually increased in the four cell lines. Because both Panc-1 and SW-1990 cells express high levels of *miR-106a*, we selected the Panc-1 and SW-1990 cell lines to explore the tumor promoting role or anti-tumor activity of *miR-106a* mimics and inhibitors, respectively.

Transfection efficiency of *miR-106a* mimics, inhibitors and controls was detected by qRT-PCR in the Panc-1 cell line (Fig. 1C). The data indicated that levels of *miR-106a* in Panc-1 cells transfected with mimics was up-regulated approximately 4.74-fold. Conversely, the level of *miR-106a* transfected with inhibitors was down-regulated approximately 0.38-fold. These findings led to the confirmation that mimics augment and inhibitors attenuate the endogenous mature level of *miR-106a*.

3.2. Promotion of cell proliferation with enforced expression of miR-106a mimics in PC cells

First, we investigated the growth promoting activity of *miR-106a* with enforced expression in PC cells by transfecting Panc-1 and SW-1990 cells with *miR-106a* mimics or negative controls.

In transfected Panc-1 cells, we found a significant increase in Panc-1 cells by the MTT assay. At 48 h post-transfection, proliferation of Panc-1 cells transfected with *miR-106a* mimics increased by 126.37 ± 7.39%. Similarly, SW-1990 cells showed a 127.77 ± 12.86% increase by enhancing endogenous *miR-106a* levels (Fig. 2B and D).

At 48 h after transfection with mimics, we also assessed changes in cell cycle distribution by flow cytometry to further explore the potential mechanism of cell proliferation in Panc-1 and SW-1990 cells (Fig. 3A and C). We observed a lower percentage of Panc-1 and SW-1990 cells in the G1-phase at 43.77 ± 3.74% and 46.32 ± 4.5%, respectively.

Following cell cycle assessment, apoptosis induced by *miR-106a* mimics was also investigated using PI and Annexin V double staining assays (Fig. 3B and D). The assays demonstrated that at 48 h post-transfection, a significantly lower apoptotic rate was found in the Panc-1 cells transfected with *miR-106a* mimics compared with their controls (1.11 ± 0.27%). A similar phenomenon was also found in SW-1990 cells (2.30 ± 0.76%).

3.3. Inhibition of proliferation with enforced expression of miR-106a inhibitors in PC cells

To investigate the potential anti-tumorigenic ability of *miR-106a* inhibitors, we transfected Panc-1 and SW-1990 cells with *miR-106a* inhibitors. Using MTT assays and flow cytometry, we found significant anti-proliferative activity induced by *miR-106a* inhibitors in both cell lines.

Results from MTT assays illustrated a significant decrease in Panc-1 and SW-1990 cells after transfection with *miR-106a* inhibitors (Fig. 2A and C). Growth inhibition in Panc-1 and SW-1990 cells transfected with inhibitors was observed in 65.91 ± 11.70% and 67.98 ± 11.08% of cells, respectively. Moreover, growth inhibition peaked at 48 h after transfection and decreased at 96 h post-transfection.

Cell cycle analysis revealed that Panc-1 cells undergo cell cycle arrest in the G1-phase after transfection (64.63 ± 8.36%). An increase of cells in the G1-phase was also detected by flow cytometry in SW-1990 cells; significant levels were attained at 48 h after transfection (65.96 ± 5.06%) (Fig. 3A and C).

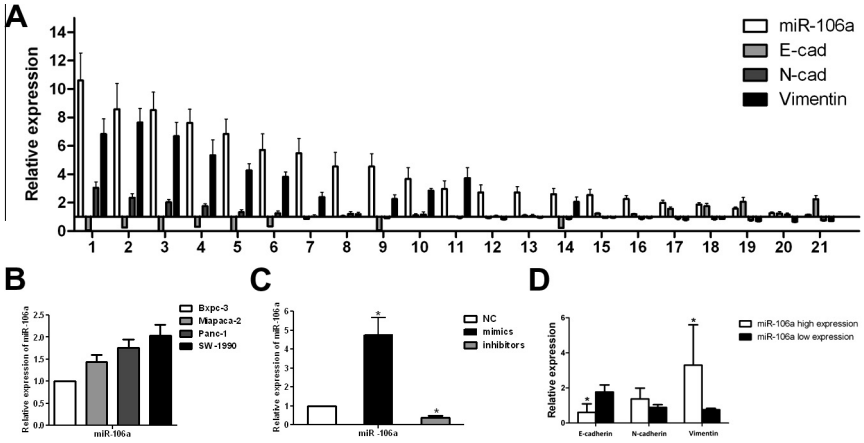

Fig. 1. Expression of genes in pancreatic cancer tissues and cell lines. (A) The ratio of relative gene expression in 21 pancreatic cancer tissues to adjacent normal pancreas tissues by qRT-PCR. (B) The relative expression of *miR-106a* in pancreatic cancer cell lines (Bxpc-3, Miapaca-2, Panc-1 and SW-1990) was detected by qRT-PCR. (C) The *miR-106a* mimics or inhibitors transfection efficiency was confirmed by qRT-PCR. The *U6* snRNA was used as an internal control. Data are expressed as mean ± SD for three separate experiments performed in duplicate (*$P < 0.05$). (D) The relative expression level of *E-cadherin*, *N-cadherin* and *vimentin* in miR-106a high expression group or miR-106a low expression group (*$P < 0.05$).

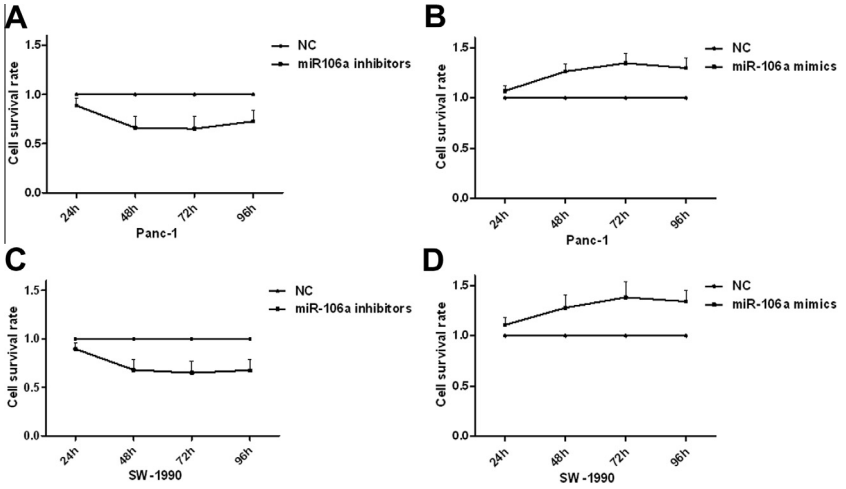

Fig. 2. Up-regulated or down-regulated *miR-106a* levels in pancreatic cancer cell lines induced growth promotion and inhibition. (A and C) MTT assay showed growth inhibition in Panc-1 and SW-1990 cells transfected with *miR-106a* inhibitors at different time points. (B and D) MTT assay showed growth promotion in Panc-1 and SW-1990 cells transfected with *miR-106a* mimics at different time points.

The apoptosis assay demonstrated that at 48 h post-transfection, a significantly higher apoptotic rate was found in the Panc-1 and SW-1990 cells transfected with miR-106a inhibitors compared with their controls (5.54 ± 1.39% in Panc-1 cells and 9.49 ± 1.89% in SW-1990 cells) (Fig. 3B and D).

3.4. MiR-106a modulates cell invasion and expression of MMPs

To further explore the positive regulatory role of *miR-106a* in cell invasion, we performed gain-of-function and loss-of-function analyses by over-expressing or suppressing *miR-106a* with mimics or inhibitors, respectively. The transwell assay showed that over-expression of *miR-106a* significantly increased cell invasion potential compared with cells treated with scrambled control oligonucleotides, whereas a knock-down of *miR-106a* decreased cell invasion (Fig. 4A and B).

We chose *MMP-2* and *MMP-9* from *MMPs* to detect whether *miR-106a* could influence invasion-related genes. Western blot analysis data showed that expression and secretion of *MMP-2* and *MMP-9* were significantly up-regulated in the mimics group but were down-regulated in the inhibitors group (Fig. 4C). Therefore, *miR-106a* is required for pancreatic cancer cell invasion.

3.5. MiR-106a could influence alterations in EMT markers

To investigate the role of *miR-106a* in EMT, we transfected *miR-106a* mimics or inhibitors into Panc-1 and SW-1990 cells for up to 96 h. After 4 days, we did not find the classical morphology change from an epithelial cobblestone-like appearance to an elongated fibroblastoid. However, we found that the enhancement of *miR-106a* in PC cells resulted in the down-regulation of the epithelial marker *E-cadherin* and the up-regulation of mesenchymal markers, including *N-cadherin* and *vimentin* protein levels (Fig. 4C). These results suggest that the overexpression of *miR-106a* might be critical for the acquisition of EMT characteristics.

Having noted that *miR-106a* could alter the expression of EMT markers in pancreatic cancer cells in culture, we wondered if this regulation also occurs in vivo. To illustrate this question, we investigated *E-cadherin*, *N-cadherin* and *vimentin* mRNA expression by qRT-PCR in PDAC tissues, in comparison with adjacent normal pancreatic tissues. The data showed that the expression level of *E-cadherin* was decreased significantly in *miR-106a* high expression group than in *miR-106a* low expression group. The expression level of *vimentin* was increased more than one-fold in *miR-106a* high expression group than in *miR-106a* low expression group. But we

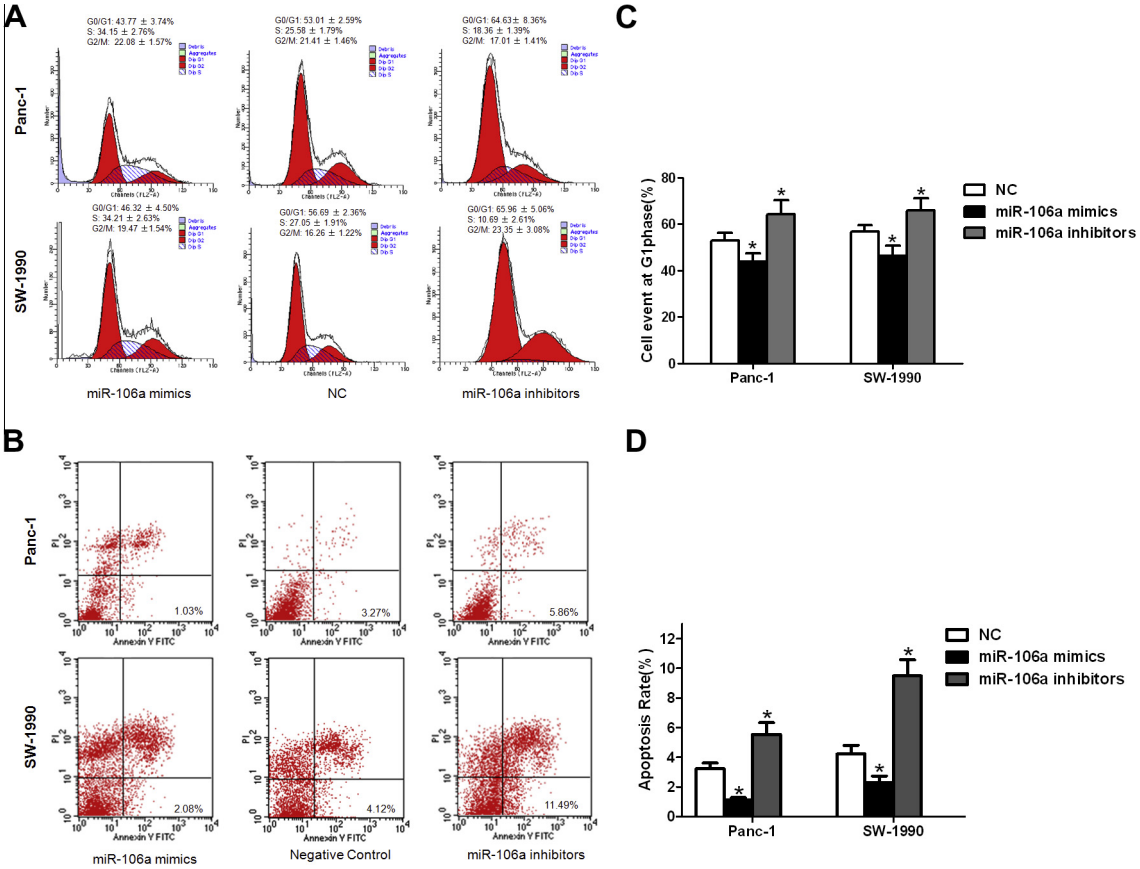

Fig. 3. Up-regulated or down-regulated *miR-106a* levels in pancreatic cancer cell lines showed cell cycle and apoptosis rate modulation. (A) Cell cycle analysis was performed by flow cytometry (FCM) in Panc-1 or SW-1990 cells 48 h after transfection of *miR-106a* mimics, inhibitors, or negative controls. (B) Cell apoptosis was analyzed by FCM in Panc-1 or SW-1990 cells 48 h after transfection of *miR-106a* mimics, inhibitors, or negative controls. (C) Graphical representation of the FCM analysis in (A). (*$P < 0.05$). The data are expressed as mean ± SD of three independent experiments. (D) Ratio of apoptosis in cells transfected with oligoribonucleotides (*$P < 0.05$). The data are expressed as mean ± S.D. of three independent experiments.

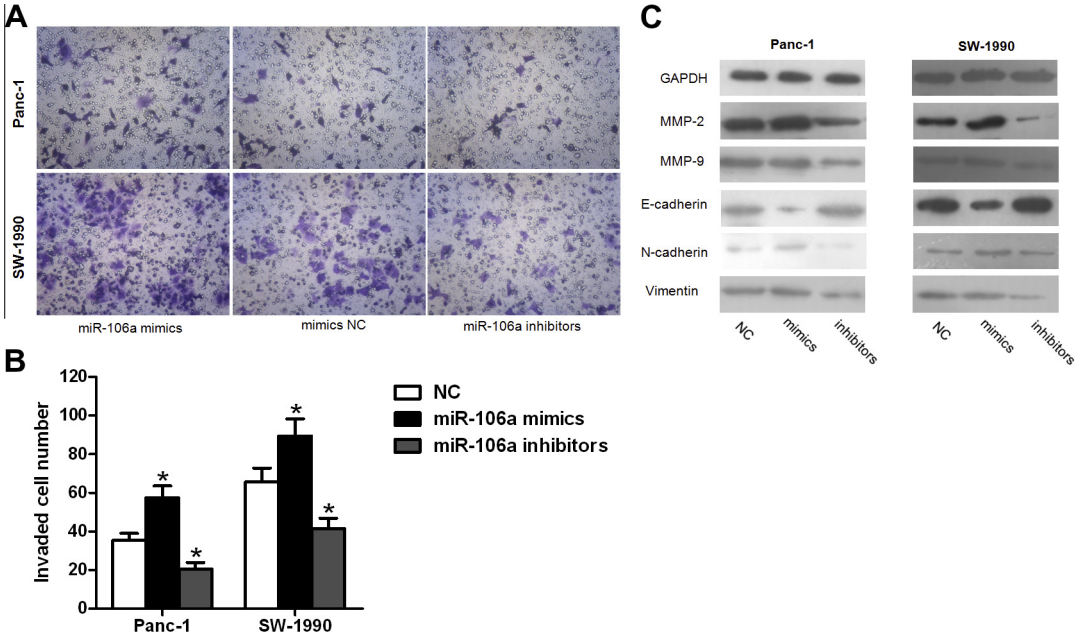

Fig. 4. *MiR-106a* promotes the invasion of pancreatic cancer cells. (A) Invasion after transfection of Panc-1 and SW-1990 cells with *miR-106a* mimics or inhibitors and their negative controls. (B) Graphical representation of the transwell assay in (A). (*$P < 0.05$). The data are expressed as mean ± S.D. of three independent experiments. (C) Cells (Panc-1 and SW-1990) were transfected with *miR-106a* mimics or negative controls, *MMP-2*, *MMP-9*, *E-cadherin*, *N-cadherin* and *Vimentin* protein levels were detected by Western blot assays. *GAPDH* protein was assayed as a control.

did not find significant association between the expression of *N-cadherin* and *miR-106a* (Fig. 1A and D).

For further clinic-pathological evaluation, the experimental samples were divided into two groups according to the expression of *miR-106a*. *E-cadherin*, *N-cadherin*, *vimentin* and *GAPDH* were analyzed by qRT-PCR for three separate experiments. Differences in gene expression were quantified based on the discrepancy between $\triangle Ct_{Ca}$ and $\triangle Ct_{Cp}$. Significantly lower expression of *E-cadherin* in pancreatic cancer tissues compared with their matched non-tumor adjacent normal pancreas tissues were assigned to negative group (*E-cad*: $n = 10$). Other *E-cadherin* expression were assigned to positive group. (*E-cad*: $n = 11$). Significantly higher expression of *N-cadherin* or *vimentin* in pancreatic cancer tissues compared with their matched non-tumor adjacent tissue were assigned to positive group (*N-cad*: $n = 11$ and *Vimentin*: $n = 12$), whereas the remaining tumors were assigned to the negative group (*N-cad*: $n = 10$ and *Vimentin*: $n = 9$). The relationship between *miR-106a* and EMT hallmarkers mRNA in pancreatic cancer is summarized in Table 2. The tumors with high *miR-106a* expression have lower *E-cadherin* ($P = 0.0351$) and higher *vimentin* ($P = 0.0062$) expression.

3.6. TIMP-2 is a direct target of miR-106a

To determine the mechanism of action of *miR-106a* in pancreatic cancer cell invasion, we performed a target search using TargetScan and found that the "seed sequence" of *miR-106a* matched the 3′UTR of the *TIMP-2* gene (Fig. 5A).

To detect whether *TIMP-2* was indeed regulated by *miR-106a* in pancreatic cancer cells, we created reporter plasmids (WT-*TIMP-2* 3′UTR or its mutant form MUT-*TIMP-2* 3′UTR). Reporter assays revealed that a reduction of *miR-106a* triggered a notable increase in luciferase activity from the WT-*TIMP-2* 3′UTR reporter plasmid (Fig. 5C).

In addition, the expression of *TIMP-2* was also detected by qRT-PCR and Western blot assays. Overexpression of *miR-106a* mimics in Panc-1 and SW-1990 cells led to a corresponding decrease of endogenous *TIMP-2* mRNA at 48 h post-transfection (Fig. 5B). Western blot analysis showed that *TIMP-2* expression was down-regulated in cells with enhanced levels of *miR-106a*, whereas *TIMP-2* expression was up-regulated in cells exhibiting a knock-down of *miR-106a* (Fig. 5D).

3.7. Inhibition of TIMP-2 mimics miR-106a-induced invasion

We succeeded in obtaining siRNA-transfected cells (Panc-1) termed *TIMP2*-homo-418, *TIMP2*-homo-754, *TIMP2*-homo-503. Western blotting showed that, compared with *TIMP2*-homo-754 and *TIMP2*-homo-503 transfected cells, the expression level of *TIMP-2* was inhibited up to 40% by transfected with *TIMP2*-homo-418 ($P < 0.05$, Fig. 6A). So, we selected the *TIMP2*-homo-418 to explore the *TIMP-2* inhibiting role or oncogene role. Compared with *miRNA-106a*, inhibition of *TIMP-2* by *TIMP2*-homo-418 was detected (Fig. 6A).

Having demonstrated *TIMP-2* is a functional target of *miR-106a* by our present study, we next transfected siRNA-*TIMP2* into Panc-1 cell. Transwell assays showed that cells transfected with siRNA-*TIMP2* had significantly promoted cell invasion (Fig. 6B).

To further investigate the role of siRNA-*TIMP2* in modulation of invasion, we explore the *MMPs* and EMT related genes expression. siRNA-*TIMP2*, *miR-106a* mimics and negative controls were transfected into Panc-1 cells for up to 96 h. Western blot analysis data showed that expression and secretion of *MMP-2* and *MMP-9* were significantly up-regulated in the siRNA-*TIMP2* group which well mimics the *miR-106a* mimics group. And EMT process was also induced by siRNA-*TIMP2* (Fig. 6C). These results indicate that *TIMP-2* is a major target of *miR-106a* in regulating pancreatic cancer cell invasion. In order to explore whether siRNA-*TIMP2* could effect proliferation of Panc-1 cells or not, we detected the proliferation rate by MTT assay. The data showed there is no significantly change by transfected with si-*TIMP2*-418 at different time points (Fig. 6D).

Table 2
Association between *miR-106a* and EMT hallmarkers mRNA expression in pancreatic cancer.

Factors		miR-106a		
		+	–	*P*
E-cad	–	10	0	0.0351*
	+	6	5	
N-cad	+	10	1	0.1486
	–	6	4	
Vimentin	+	12	0	0.0062*
	–	4	5	

Statistical analysis was performed using Fisher exact test.
* $P < 0.05$.

4. Discussion

In previous studies, *miR-106a* expression was found to be slightly down-regulated in breast tumor samples [19] and significantly lower in astrocytoma and glioma [17,20]. However, little information is known with respect to the relevance of *miR-106a* in pancreatic cancer. To investigate levels of *miR-106a* expression and the role of *miR-106a* in pancreatic cancer, we conducted our study using pancreatic cancer tissues and four pancreatic cancer cell lines. qRT-PCR analysis showed that *miR-106a* was overexpressed compared with adjacent benign tissues and increased with enhanced cell invasiveness. SW-1990, a highly invasive pancreatic cancer cell line, exhibited the highest level of *miR-106a* of the four cell lines, which could indicate that overexpression of *miR-106a* may be involved in pancreatic cancer invasion. In studies conducted by Wang and Ivkovic et al. [12,13], *miR-106a* was found to be an oncogene in gastric and colorectal cancers.

MiR-106a plays two roles in the development of tumors; Wang et al. found that *miR-106a* could inhibit the extrinsic apoptotic pathway by targeting the *FAS* cell surface receptor to further promote cell proliferation and repress apoptosis. Conversely, Yang et al. [17] presented data showing *miR-106a* as a negative regulator of glioma progression by interacting with *E2F1* to inhibit cell proliferation and induce apoptosis. Hence, our aim was to explore the role of *miR-106a* in pancreatic cancer.

Following transfection, endogenous levels of *miR-106*a were up-regulated or down-regulated by mimics or inhibitors, respectively. MTT assay results showed significant alterations in the proliferation of transfected cells. Subsequent to transfection with *miR-106a* inhibitors, cell viability was significantly reduced, thereby inhibiting cell growth. However, cells transfected by *miR-106a* mimics exhibited stimulation of tumor cell growth.

Cell cycle aberration is an essential step in carcinogenesis [21]. We further explored changes in cell cycle profile. The FCM results indicated that a reduction of *miR-106a* induced cell cycle arrest in the G1 phase in Panc-1 and SW-1990 cells. *RB1*, a tumor suppressor and negative regulator of cell cycle progression, was identified in other studies [22–24]. Interestingly, *RB1* was confirmed as a direct target of *miR-106a* by Jiang and Ivkovic et al. [8,12]. Therefore, *miR-106a* may affect the cell cycle in pancreatic cancer through *RB1* knockdown. Further study will be necessary to confirm the relationship between *miR-106a* and *RB1*. Considering that *RB1* does not merely influence cell cycle but also apoptosis, we used FCM to analyze cellular apoptosis after treatment with *miR-106a* mimics

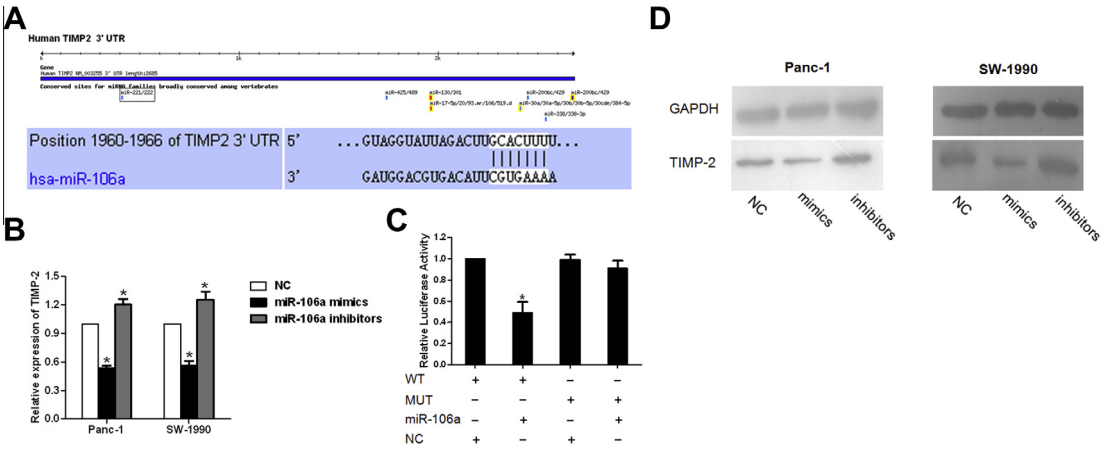

Fig. 5. Regulation of *TIMP-2* by *miR-106a*. (A) Software prediction of *miR-106a* a potential binding sites on *TIMP-2* 3′-UTR. The nucleotide sequence illustrates the predicted base-pairing between *miR-106a* and *TIMP-2* 3′-UTR. (B) The relative level of *TIMP-2* mRNA was determined by the qRT-PCR (*$P < 0.05$). The data are the mean ± S.D. of three independent experiments. (C) Luciferase activity was assayed at 48 h post-transfection. The firefly luciferase activity of each sample was normalized by the Renilla luciferase activity (*$P < 0.05$). The data are the mean ± S.D. of three independent experiments. (D) The expression of *TIMP-2* protein was detected by Western blot. GAPDH protein was assayed as a control.

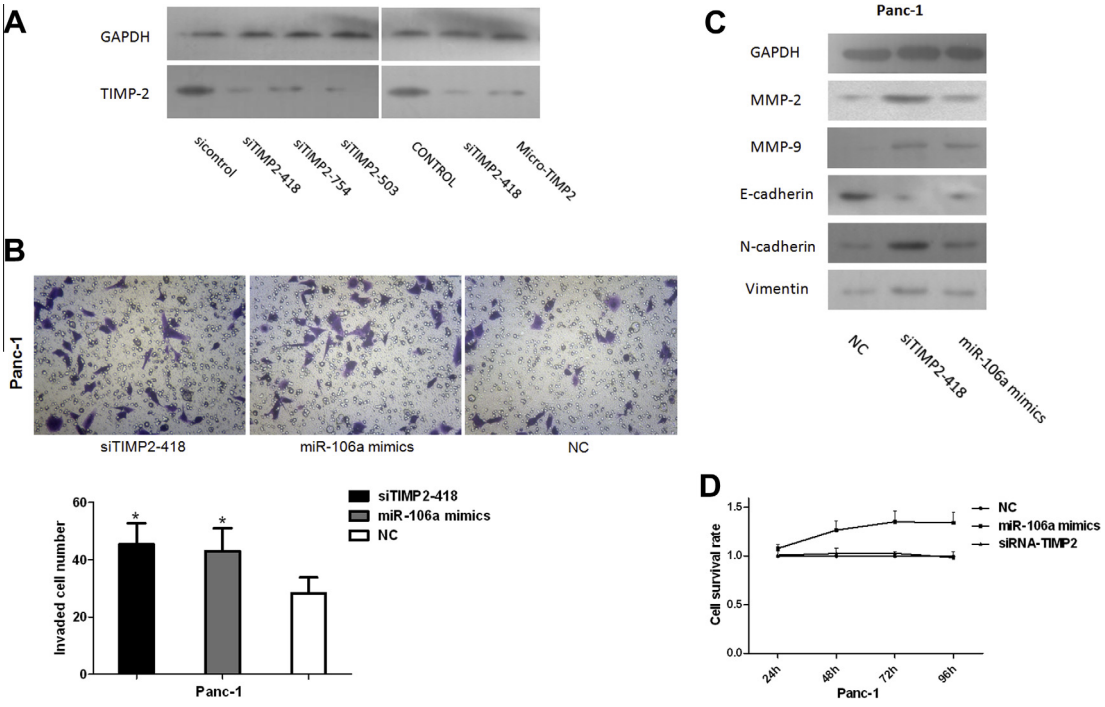

Fig. 6. *TIMP-2* inhibition could mimics *miR-106a* in promoting cell invasion. (A) si*TIMP2*-418 could inhibit expression of *TIMP-2*. (B) Inhibition of *TIMP-2* by si*TIMP2*-418 mimics *miR-106a*-induced invasion. (*$P < 0.05$). (C) Panc-1 cells were transfected with si*TIMP2*-418, *miR-106a* mimics and negative controls, *MMP-2*, *MMP-9*, *E-cadherin*, *N-cadherin* and *Vimentin* protein levels were detected by Western blot assays. *GAPDH* protein was assayed as a control. (D) MTT assay showed there is no significantly change by transfected with si*TIMP2*-418 at different time points.

or inhibitors. Flow cytometry analysis depicted a promotion of apoptosis by blocking endogenous *miR-106a* in both Panc-1 and SW-1990 cells, whereas enhancing the endogenous levels of *miR-106a* suppressed apoptosis to promote cell survival.

The oncogenic role of *miR-106a* was evaluated by the transwell assay, which showed that *miR-106a* could positively influence the invasiveness of pancreatic cancer cells. As critical indicators of cell invasiveness, our attention was drawn to *MMP-2* and *MMP-9*. We detected that *MMP-2* and *MMP-9* were up-regulated or down-regulated in cells treated with *miR-106a* mimics or inhibitors, respectively. The results imply that pancreatic cancer cell invasion was dependent on *miR-106a* regulation.

Several genes have been found to be common targets of miR-106a, such as *RB1*, *FAS*, *E2F1* and *TGFBR2* [12,13,17,25]. Our data demonstrated that *miR-106a* plays a critical role in the regulation of pancreatic cancer invasion by directly targeting *TIMP-2*, an inhibitor of *MMPs*. Among the *MMPs*, *MMP-2* and *MMP-9* were implicated in human cancer invasion [26–28]. A major mechanism for controlling the activity of *MMPs* is mediated by the action of tissue inhibitors of metalloproteinases (*TIMPs*) [29]. The imbalance between *MMPs* and *TIMPs* is crucial for many physiological processes in tissue, including tumor microenvironment [30]. *TIMP-2*, a member of the *TIMP* gene family, was determined to be a functional target of *miR-106a* by the dual luciferase 3′UTR-reporter

and Western blot assays in our study. Moreover, when successfully blocking *TIMP-2* expression, we could get the similar result with *miR-106a*. These results demonstrate that *TIMP-2* is a core target of *miR-106a* in pancreatic cancer cell invasion.

In recent years, it has become increasingly clear that EMT plays an important role in the progression of cancer and could also be responsible for invasion and metastasis. Up to now, many miRNAs have been considered connected to EMT [31–33]. To clarify whether *miR-106a* participates in EMT to enhance pancreatic cancer cell invasiveness, we detected three hallmarks of EMT. *E-cadherin* levels were diminished after treatment with *miR-106a* mimics. Conversely, mesenchymal markers *N-cadherin* and *vimentin* were enhanced. Moreover, we detected the three hallmarks in vitro, the data showed the relative expression level of *E-cadherin* and *vimentin* were significantly associated with the expression of miR-106a. In a study of colorectal cancer by Feng et al. [25], the expression level of *miR-106a* in colorectal cancer cell lines was demonstrated to be associated with EMT. Therefore, we conclude *miR-106a* could induce EMT to promote pancreatic cancer invasion.

Overall, we demonstrate that a high level of *miR-106a* expression was found in pancreatic cancer. Furthermore, our investigation shows that *miR-106a* has an oncogenic role in pancreatic tumorigenesis by promoting cancer cell proliferation, epithelial–mesenchymal transition and invasion by targeting *TIMP-2*. These findings confirm that *miR-106a* could be a critical therapeutic target in pancreatic cancer.

Acknowledgements

We thank Professor Chen Huang (Department of genetics and Molecular Biology, Medical School, Xi'an Jiaotong university/ key laboratory of environment and genes related to diseases, Ministry of education, Xi'an, China) for his thoughtful reading of the manuscript. The study was supported by National Natural Science Foundation of China (No. 81201824); the Fundamental Research Funds for the Central Universities in Xi'an Jiaotong University.

References

[1] Calin, G.A. and Croce, C.M. (2006) MicroRNA signatures in human cancers. Nat. Rev. Cancer 6, 857–866.
[2] Michael, M.Z., O' Connor, S.M., van Holst Pellekaan, N.G., Young, G.P. and James, R.J. (2003) Reduced accumulation of specific microRNAs in colorectal neoplasia. Mol. Cancer Res. 1, 882–891.
[3] Calin, G.A., Liu, C.G., Sevignani, C., Ferracin, M., Felli, N., Dumitru, C.D., Shimizu, M., Cimmino, A., Zupo, S., Dono, M., Dell'Aquila, M.L., Alder, H., Rassenti, L., Kipps, T.J., Bullrich, F., Negrini, M. and Croce, C.M. (2004) MicroRNA profiling reveals distinct signatures in B cell chronic lymphocytic leukemias. Proc. Natl. Acad. Sci. U S A 101, 11755–11760.
[4] Takamizawa, J., Konishi, H., Yanagisawa, K., Tomida, S., Osada, H., Endoh, H., Harano, T., Yatabe, Y., Nagino, M., Nimura, Y., Mitsudomi, T. and Takahashi, T. (2004) Reduced expression of the let-7 microRNAs in human lung cancers in association with shortened postoperative survival. Cancer Res. 64, 3753–3756.
[5] Lu, J., Getz, G., Miska, E.A., Alvarez-Saavedra, E., Lamb, J., Peck, D., Sweet-Cordero, A., Ebert, B.L., Mak, R.H., Ferrando, A.A., Downing, J.R., Jacks, T., Horvitz, H.R. and Golub, T.R. (2005) MicroRNA expression profiles classify human cancers. Nature 435, 834–838.
[6] Zhang, C., Zhang, J., Hao, J., Shi, Z., Wang, Y., Han, L., Yu, S., You, Y., Jiang, T., Wang, J., Liu, M., Pu, P. and Kang, C. (2012) High level of miR-221/222 confers increased cell invasion and poor prognosis in glioma. J. Transl. Med. 10, 119.
[7] Srivastava, S.K., Bhardwaj, A., Singh, S., Arora, S., Wang, B., Grizzle, W.E. and Singh, A.P. (2011) MicroRNA-150 directly targets MUC4 and suppresses growth and malignant behavior of pancreatic cancer cells. Carcinogenesis 32, 1832–1839.
[8] Jiang, Y., Wu, Y., Greenlee, A.R., Wu, J., Han, Z., Li, X. and Zhao, Y. (2011) MiR-106a-mediated malignant transformation of cells induced by anti-benzo[a]pyrene-trans-7,8-diol-9,10-epoxide. Toxicol. Sci. 119, 50–60.
[9] Ali, S., Ahmad, A., Banerjee, S., Padhye, S., Dominiak, K., Schaffert, J.M., Wang, Z., Philip, P.A. and Sarkar, F.H. (2010) Gemcitabine sensitivity can be induced in pancreatic cancer cells through modulation of miR-200 and miR-21 expression by curcumin or its analogue CDF. Cancer Res. 70, 3606–3617.
[10] Wang, F., Xue, X., Wei, J., An, Y., Yao, J., Cai, H., Wu, J., Dai, C., Qian, Z., Xu, Z. and Miao, Y. (2010) Hsa-miR-520h downregulates ABCG2 in pancreatic cancer cells to inhibit migration, invasion, and side populations. Br. J. Cancer 103, 567–574.
[11] Cui, L., Zhang, X., Ye, G., Zheng, T., Song, H., Deng, H., Xiao, B., Xia, T., Yu, X., Le, Y. and Guo, J. (2013) Gastric juice MicroRNAs as potential biomarkers for the screening of gastric cancer. Cancer 119, 1618–1626.
[12] Catela Ivkovic, T., Aralica, G., Cacev, T., Loncar, B. and Kapitanovic, S. (2013) miR-106a overexpression and pRB downregulation in sporadic colorectal cancer. Exp. Mol. Pathol. 94, 148–154.
[13] Wang, Z., Liu, M., Zhu, H., Zhang, W., He, S., Hu, C., Quan, L., Bai, J. and Xu, N. (2013) MiR-106a is frequently upregulated in gastric cancer and inhibits the extrinsic apoptotic pathway by targeting FAS. Mol. Carcinog. 52, 634–646.
[14] Tsujiura, M., Ichikawa, D., Komatsu, S., Shiozaki, A., Takeshita, H., Kosuga, T., Konishi, H., Morimura, R., Deguchi, K., Fujiwara, H., Okamoto, K. and Otsuji, E. (2010) Circulating microRNAs in plasma of patients with gastric cancers. Br. J. Cancer 102, 1174–1179.
[15] Schetter, A.J., Leung, S.Y., Sohn, J.J., Zanetti, K.A., Bowman, E.D., Yanaihara, N., Yuen, S.T., Chan, T.L., Kwong, D.L., Au, G.K., Liu, C.G., Calin, G.A., Croce, C.M. and Harris, C.C. (2008) MicroRNA expression profiles associated with prognosis and therapeutic outcome in colon adenocarcinoma. JAMA 299, 425–436.
[16] Link, A., Balaguer, F., Shen, Y., Nagasaka, T., Lozano, J.J., Boland, C.R. and Goel, A. (2010) Fecal MicroRNAs as novel biomarkers for colon cancer screening. Cancer Epidemiol. Biomarkers Prev. 19, 1766–1774.
[17] Yang, G., Zhang, R., Chen, X., Mu, Y., Ai, J., Shi, C., Liu, Y., Shi, C., Sun, L., Rainov, N.G., Li, H., Yang, B. and Zhao, S. (2011) MiR-106a inhibits glioma cell growth by targeting E2F1 independent of p53 status. J. Mol. Med. (Berlin) 89, 1037–1050.
[18] Chen, C., Ridzon, D.A., Broomer, A.J., Zhou, Z., Lee, D.H., Nguyen, J.T., Barbisin, M., Xu, N.L., Mahuvakar, V.R., Andersen, M.R., Lao, K.Q., Livak, K.J. and Guegler, K.J. (2005) Real-time quantification of microRNAs by stem-loop RT-PCR. Nucleic Acids Res. 33, e179.
[19] Volinia, S., Calin, G.A., Liu, C.G., Ambs, S., Cimmino, A., Petrocca, F., Visone, R., Iorio, M., Roldo, C., Ferracin, M., Prueitt, R.L., Yanaihara, N., Lanza, G., Scarpa, A., Vecchione, A., Negrini, M., Harris, C.C. and Croce, C.M. (2006) A microRNA expression signature of human solid tumors defines cancer gene targets. Proc. Natl. Acad. Sci. U S A 103, 2257–2261.
[20] Zhi, F., Chen, X., Wang, S., Xia, X., Shi, Y., Guan, W., Shao, N., Qu, H., Yang, C., Zhang, Y., Wang, Q., Wang, R., Zen, K., Zhang, C.Y., Zhang, J. and Yang, Y. (2010) The use of hsa-miR-21, hsa-miR-181b and hsa-miR-106a as prognostic indicators of astrocytoma. Eur. J. Cancer 46, 1640–1649.
[21] Malumbres, M. and Barbacid, M. (2001) To cycle or not to cycle: a critical decision in cancer. Nat. Rev. Cancer 1, 222–231.
[22] Friend, S.H., Bernards, R., Rogelj, S., Weinberg, R.A., Rapaport, J.M., Albert, D.M. and Dryja, T.P. (1986) A human DNA segment with properties of the gene that predisposes to retinoblastoma and osteosarcoma. Nature 323, 643–646.
[23] Burkhart, D.L. and Sage, J. (2008) Cellular mechanisms of tumour suppression by the retinoblastoma gene. Nat. Rev. Cancer 8, 671–682.
[24] Indovina, P., Marcelli, E., Casini, N., Rizzo, V. and Giordano, A. (2013) Emerging roles of RB family: new defense mechanisms against tumor progression. J. Cell Physiol. 228, 525–535.
[25] Feng, B., Dong, T.T., Wang, L.L., Zhou, H.M., Zhao, H.C., Dong, F. and Zheng, M.H. (2012) Colorectal cancer migration and invasion initiated by microRNA-106a. PLoS One 7, e43452.
[26] Rogers, A., Smith, M.J., Doolan, P., Clarke, C., Clynes, M., Murphy, J.F., McDermott, A., Swan, N., Crotty, P., Ridgway, P.F. and Conlon, K.C. (2012) Invasive markers identified by gene expression profiling in pancreatic cancer. Pancreatology 12, 130–140.
[27] Liu, J., Ben, Q.W., Yao, W.Y., Zhang, J.J., Chen, D.F., He, X.Y., Li, L. and Yuan, Y.Z. (2012) BMP2 induces PANC-1 cell invasion by MMP-2 overexpression through ROS and ERK. Front. Biosci. 17, 2541–2549.
[28] Durlik, M. and Gardian, K. (2012) Metalloproteinase 2 and 9 activity in the development of pancreatic cancer. Pol. Przegl. Chir. 84, 377–382.
[29] Kessenbrock, K., Plaks, V. and Werb, Z. (2010) Matrix metalloproteinases: regulators of the tumor microenvironment. Cell 141, 52–67.
[30] Gong, Y.L., Xu, G.M., Huang, W.D. and Chen, L.B. (2000) Expression of matrix metalloproteinases and the tissue inhibitors of metalloproteinases and their local invasiveness and metastasis in Chinese human pancreatic cancer. J. Surg. Oncol. 73, 95–99.
[31] Chen, Y., Xiao, Y., Ge, W., Zhou, K., Wen, J., Yan, W., Wang, Y., Wang, B., Qu, C., Wu, J., Xu, L. and Cai, W. (2013) MiR-200b inhibits TGF-beta1-induced epithelial–mesenchymal transition and promotes growth of intestinal epithelial cells. Cell Death Dis. 4, e541.
[32] Paterson, E.L., Kazenwadel, J., Bert, A.G., Khew-Goodall, Y., Ruszkiewicz, A. and Goodall, G.J. (2013) Down-regulation of the miRNA-200 family at the invasive front of colorectal cancers with degraded basement membrane indicates EMT is involved in cancer progression. Neoplasia 15, 180–191.
[33] Martello, G., Rosato, A., Ferrari, F., Manfrin, A., Cordenonsi, M., Dupont, S., Enzo, E., Guzzardo, V., Rondina, M., Spruce, T., Parenti, A.R., Daidone, M.G., Bicciato, S. and Piccolo, S. (2010) A MicroRNA targeting dicer for metastasis control. Cell 141, 1195–1207.